

2.2.3.- X-ray diffraction

2.2.3.1.- Origins and fundamentals of the technique

The first experimental evidence concerning x-ray diffraction was given by Max von Laue who in 1912 demonstrated that x-rays could have a comparable wavelength to the atomic spacing in crystals and, therefore, they could be diffracted [36]. This was immediately confirmed by Walter Friedrich and Paul Knipping [36].

In 1914 Darwin elaborated a Kinematic Theory of Diffraction, which assumed that x-rays diffracted by each element in the volume of the material were independent of x-rays diffracted by the other elements [37]. Once diffracted, the beam could not be diffracted again by other elements. Two years later Ewald proposed the Dynamical Theory of Diffraction, which took into account the possibility of having more than one reflection inside the material before the beam emerged from it [38].

If one assumes that the incident x-ray beam is perfectly collimated and monochromatic (with a single wavelength λ) and makes an incident angle θ with respect to the reticular planes of the crystal, it can be demonstrated (see appendix I) that when the following condition is fulfilled:

$$n\lambda = 2d \sin\theta \quad (2.3)$$

where n is the reflection order and d is the interplanar distance of one family of crystallographic planes, x-rays will be completely in phase and will, therefore, give constructive interferences. This condition is known as *Bragg's law* and it can be used to determine the angular positions of the XRD peaks diffracted by each family of planes [39,40,41].

The Bragg's law assumes the crystal is ideal (without structural defects) and the incident beam is perfectly monochromatic and collimated. These conditions are never fulfilled completely. Moreover, usually, the particles are found to be composed of several grains, with different orientation and with certain amount of defects. Each of these grains is called a *crystallite*. The size of these crystallites and the microstrains present in them can also be obtained from the XRD spectra, since both effects contribute to the width of the diffraction peaks [40,41]. The most frequent procedure to evaluate these effects is to consider that the peaks can be fitted using a pseudo-Voigt function (see appendix I), which is a linear

combination of a gaussian and a lorentzian (or Cauchy) profile [42,43]. Using this formalism, the crystallite size can be deduced from the Cauchy contribution to the integral width of the diffraction peak, \mathbf{b}_{fC} , as follows:

$$d_{hkl} = \frac{\mathbf{I}}{\mathbf{b}_{fC} \cos \mathbf{q}_B} \quad (2.4)$$

where \mathbf{q}_B is the angular position of the peak (measured in radians) and \mathbf{I} is the wavelength (measured in Å). The value of d_{hkl} represents the coherent diffraction domain and is measured also in Å. This equation is commonly known as the *Scherrer formula* [44]. Analogously, microstrains can be determined from the Gaussian contribution to the integral peak width, \mathbf{b}_{fG} , using the expression:

$$\text{microstrain} = \langle e \rangle = \frac{\mathbf{b}_{fG}}{4tg\mathbf{q}_B} \quad (2.5)$$

where $\langle e \rangle$ represents the upper limit of microstrains. However, it is more frequent to use the mean square root of microstrains, $\langle \mathbf{e}^2 \rangle^{1/2}$ (*rms strain*), which is related to $\langle e \rangle$ in the following way: $\langle e \rangle = 1.25 \langle \mathbf{e}^2 \rangle^{1/2}$. Deduction of equations 2.4 and 2.5 and a detailed description of the methods used in this work to fit the XRD data is presented in appendix I.

When a powder sample, composed of several phases, is analyzed by x-ray diffraction, each phase originates its own diffraction pattern. The relative intensity of the several peaks in the pattern depends on the relative concentration of the different phases. The phase identification can be carried out by comparison with the *Powder Diffraction Files* database [45].

In general, a powder diffractometer is composed of the following parts [40,41]:

- X-ray generator
- Monochromator.
- Entrance *Soller* slits
- Divergence slits
- Sample
- Exit *Soller* slits
- Reception slits
- Detector

- a) The x-ray generator is based on the impacts between source electrons and metal atoms, which result in the emission of electrons of the metal, leaving a large number of holes inside the inner electronic shells. These holes become immediately occupied by electrons from more external shells and the excess of energy is liberated as x-ray radiation, whose energy depends on the energy difference between the energy levels of the electrons and, hence, has discrete values.
- b) The monochromator is a filter used to make the radiation as monochromatic as possible, eliminating unwanted radiations.
- c) The x-ray generator emits radiation in all directions. The entrance *Soller* slits are used to obtain a parallel and collimated beam. This is accomplished by several fine metallic foils, very close to each other that are located parallel to the diffraction circle plane.
- d) There are two divergence slits that are located in front of and behind the *Soller* slits. Their role is to allow the emitted x-rays to diverge as little as possible, in an angle that can usually vary between $(1/30)^\circ$ and 4° .
- e) The sample in general needs to be flat, so that x-rays can be well focussed on its surface.
- f) The exit *Soller* slits have a similar role to the entrance *Soller* slits, i.e. to keep the diffracted beam, to some extent, collimated.
- g) The divergence slits are used to make the x-rays diffracted by the sample more convergent. The width of these slits determines the maximum intensity in the detector.
- h) There are several types of detectors: gas, Geiger, semiconductors, etc. The detectors are calibrated so as to count the number of photons per second, so that the intensities are relative to each specific equipment.

2.2.3.2.- Experimental method and working conditions

XRD experiments were carried out at the *Servei de Difracció* at the *Universitat Autònoma de Barcelona*, using a *Phillips PW3050* diffractometer.

For XRD experiments, the powders were spread on a circular PVC holder. The amount of powder was minimized so that a final thickness of about $100\text{ }\mu\text{m}$ was finally obtained. With this thickness it is possible to guarantee that there are no transparency effects, which might give XRD peaks from the holder. It is also important to have a sample surface as flat as possible. The powders were fixed onto the holders by slightly pressing them. Only occasionally some silicon grease was also required.

Some technical specifications are presented here:

Tube:*Anticathode:* Cu*Voltage:* 40 kV*Current:* 50 mA

Radiation: Cu- $K_{\alpha 1}$ $I(K_{\alpha 1}) = 1.54060 \text{ \AA}$
 $I(K_{\alpha 2}) = 1.54439 \text{ \AA}$
 $I(K_{\alpha 2}) / I(K_{\alpha 1}) = 0.500$

Primary beam optics:*Soller slits:* 0.04 mm*Divergence at the entrance:* $\frac{1}{2}^\circ$ Secondary beam optics:*Soller slits:* 0.04 mm*Divergence at the exit:* $\frac{1}{2}^\circ$ *Monochromator:* pyrolytic graphite

The x-ray spectra were obtained in a *step-scan* mode. This means that the sample and the detector rotated in steps instead of in a continuous way. The appropriate step size for each experiment was selected in order to have at least 10 experimental points above the half height width. Therefore, depending on the peak widths, $2\mathbf{q}$ steps of 0.04° or 0.08° were chosen. Moreover, the time for step was selected to be relatively long (10 to 20 s) in order to reduce the statistical error.

The powder diffractometer used in our study was set up in a *Bragg-Brentano* geometry (see fig. 2.4). In this geometry, both the x-ray source and the detector are located in the focalization circle. Since the detector has to follow the diffracted radiation, when the sample rotates at an angular speed \mathbf{w} , the detector has to rotate at $2\mathbf{w}$. Thus, if the sample rotates an angle \mathbf{q} the diffracted beam is deviated $2\mathbf{q}$ with respect to the incident direction. As a consequence, the *Bragg-Brentano* geometry is also known as “ \mathbf{q} - $2\mathbf{q}$ scan”.

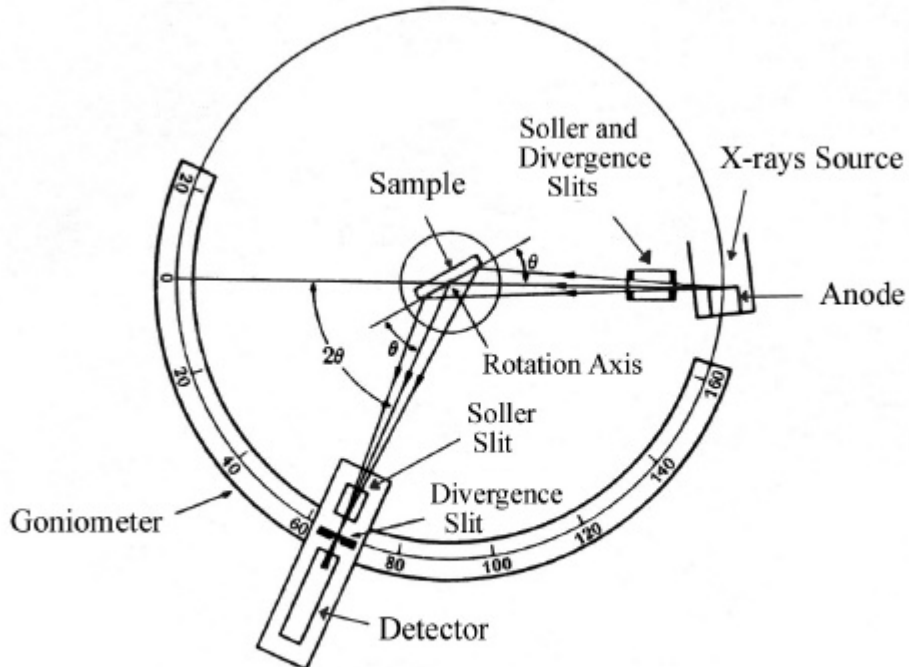


Figure 2.4: Schematic picture of a x-ray diffractometer

2.2.4.- Magnetometry Techniques

Two different types of magnetometers have been used in this work. Hysteresis loops of Co powders milled alone or with NiO or FeS were carried out using a vibrating sample magnetometer (VSM) with a maximum applied magnetic field of 11 kOe. However, due to the limited magnetic field range, SmCo₅ powders (either milled alone or with AFM powders) could not be saturated in the VSM and, therefore, it was necessary to use an extracting magnetometer located at the Grenoble High Magnetic Field Laboratory (GHMFL), with which the magnetic field could reach values in excess of 200 kOe.

Note that the system of magnetic units used in this thesis and some technical definitions of some of the magnetic properties discussed are given in appendix II.